

## Preparation of Lithium Disilicate Glass-Ceramics as Dental Bridge Material

Z. Khalkhali<sup>1</sup>, B. Eftekhari Yekta<sup>\*1</sup>, V.K. Marghussian<sup>1</sup>

<sup>1</sup>Ceramics Division, Department of Materials, Iran University of Science and Technology, Narmak, Tehran 16846–13114, Iran

received October 19, 2013; received in revised form January 26, 2014; accepted February 18, 2014

### Abstract

Sintering and crystallization behaviors of three lithium-silicate-based glass compositions were determined by heating the pressed specimens above their DTA crystallization peak temperatures.

The crystallization procedure and microstructure of the heat-treated specimens were investigated by means of differential thermal analysis, X-ray diffraction and scanning electron microscopy.

According to the results, while  $P_2O_5$  encouraged the crystallization of both  $Li_2SiO_3$  and  $Li_2Si_2O_5$  phases,  $ZrO_2$  did not show such capability. Furthermore, while  $Li_2SiO_3$  was crystallized directly as the result of a bulk crystallization mechanism,  $Li_2Si_2O_5$  tended to crystallize epitaxially on the surface of the previously precipitated  $Li_2SiO_3$  particles.

*Keywords:* Lithium disilicate, glass ceramic, dental

### I. Introduction

Since the 1990s, efforts have been made to develop bio-materials for restorative dentistry based on the production of metal-free systems<sup>1,2</sup>. Lithium disilicate ( $Li_2Si_2O_5$ ) glass ceramics with major uses in all-ceramic restorative dentistry were produced for the first time in 1995<sup>2</sup>. This material is suitable for fabricating restorative prostheses of any kind, from dental inlays, onlays, veneers and crowns to multi-unit bridges, mainly owing to its desirable strength and fracture toughness<sup>1–10</sup>, which are essential properties in dental materials as they guarantee the long lifetime of the restoration against various mechanical and thermal stresses. These properties can be achieved with certain microstructural modifications like uniform distribution of crystalline phase in the glass matrix and interlocking of needle and plate-like lithium disilicate crystals<sup>5,11,12</sup>, which can be obtained only with the bulk crystallization mechanism.

The principal method of producing multi-unit bridges is based on the viscous flow of a glass specimen, consisting of sintering of a compacted powder frit, or melt casting, and then hot pressing of the resulting glassy ingots into a lost-wax mould<sup>1</sup>.

Like other glass-ceramics, lithium disilicate glass-ceramics need suitable nucleating agents for bulk crystallization. Precious metals, e.g. Ag, Cu, and Pt, and oxides like  $ZrO_2$  and  $P_2O_5$ , with no undesirable coloring effects, seem suitable in this respect<sup>11–13</sup>. In the present work the above-mentioned oxides were adopted as nucleants and their effects on the sintering and crystallization behaviors of the

compacted bodies were compared. These behaviors have not yet been studied sufficiently for this glass system.

### II. Experimental Procedure

The chemical compositions of the prepared glasses are shown in Table 1. Reagent grade  $SiO_2$  (acid-washed, purity  $\geq 99\%$ ),  $Al_2O_3$  (MR70),  $Li_2CO_3$  (Merck, 1.05671),  $KNO_3$  (Merck, 1.05061),  $P_2O_5$  (Merck, 1.00540),  $H_3BO_3$  (Merck, 1.05061) and  $ZrO_2$  (Merck, 1.00757) powders were used as raw materials. The glass compositions were melted in high-alumina crucibles in an electric furnace, at 1350 °C for 1 h. The obtained glass melts were cooled rapidly by quenching into distilled water.

**Table 1:** Chemical compositions of the three glasses.

Constituent (wt%)	$G_B$	$G_{BZ}$	$G_P$
$SiO_2$	74.2	74.2	74.2
$Al_2O_3$	3.54	3.54	3.54
$Li_2O$	15.40	15.40	15.40
$K_2O$	3.25	3.25	3.25
$P_2O_5$	-	-	3.37
$B_2O_3$	3.37	3.37	-
$ZrO_2$	-	3.37	-

Then the resulting frits were fast-milled to particle sizes smaller than 75  $\mu m$ . Subsequently, cylindrical specimens measuring 4.5 mm in height and 15 mm in diameter were pressed at a pressure of 45 MPa.

\* Corresponding author: [beftekhari@iust.ac.ir](mailto:beftekhari@iust.ac.ir)

The compacted powders were sintered in the range 800–900 °C for 2 h. The optimum sintered specimens (ingots) were then re-fired at 950 °C for 15 min instead of the usual heat-pressing operation, which is the required procedure for shaping the final restorative.

The crystallization mechanism, crystallinity and microstructure of the sintered specimens were investigated respectively by means of differential thermal analysis (STA, Polymer Laboratories 1640), X-ray diffraction (Jeol-JDX 8030) and scanning electron microscopy (Philips XL30) techniques. Differential thermal analysis was performed with a heating rate of 10 °K/min in air atmosphere and the XRD patterns were recorded for two theta values from 5° to 80° with a step size of 0.02°. The accuracy of the XRD analyzer in determination of the d-spacing of the crystalline phases was  $\pm 0.02$ . The microstructures were evaluated via polishing and then etching of the specimens in 5 % HF for 30 s.

### III. Results and Discussion

#### (1) Sintering and crystallization behaviours of glasses

Fig. 1 shows the DTA traces of the glasses. Accordingly, while the DTA curves of  $G_B$  and  $G_{BZ}$  show a single exothermic peak, there are two peaks in the  $G_P$  thermograph. Endothermic peaks at 944, 934 and 950 °C, respectively, in the thermographs of glasses  $G_B$ ,  $G_{BZ}$  and  $G_P$  can be attributed to their liquidus temperatures. Furthermore, the dilatometric softening points ( $T_s$ ) of glasses  $G_B$  and  $G_P$  are about 465 °C and that of  $G_{BZ}$  is about 490 °C. This means that  $ZrO_2$  has increased the viscosity and so the crystallization temperature of  $G_{BZ}$ . In addition, comparison of the glasses shows that  $G_P$  exhibits a higher peak intensity than the other glasses, which means it has been crystallized more extensively during the DTA run.

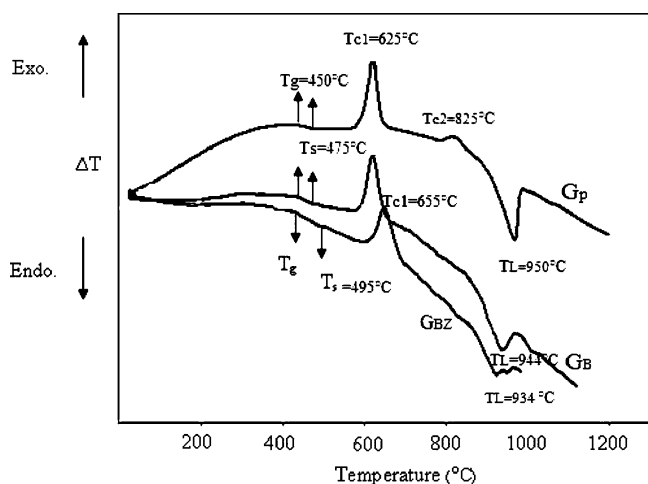


Fig. 1: DTA traces of glasses.

Fig. 2 shows the X-ray diffraction patterns of the  $G_P$  glasses, after heat treatment at their first and the second crystallization peak temperatures for 2 h. Accordingly, the first peak in the DTA traces represents the crystallization of lithium metasilicate ( $Li_2SiO_3$ ) and the second one, which only emerges in the DTA curve of specimen  $G_P$  at 825 °C, represents the crystallization of lithium disilicate ( $Li_2Si_2O_5$ ). Crystallization of  $Li_2Si_2O_5$  in  $G_B$  and  $G_{BZ}$  during the heat treatment at 825 °C and the lack of a

distinctive second exothermic peak in their DTA thermographs mean that surface crystallization is the dominant mechanism for the crystallization of  $Li_2Si_2O_5$  in them.

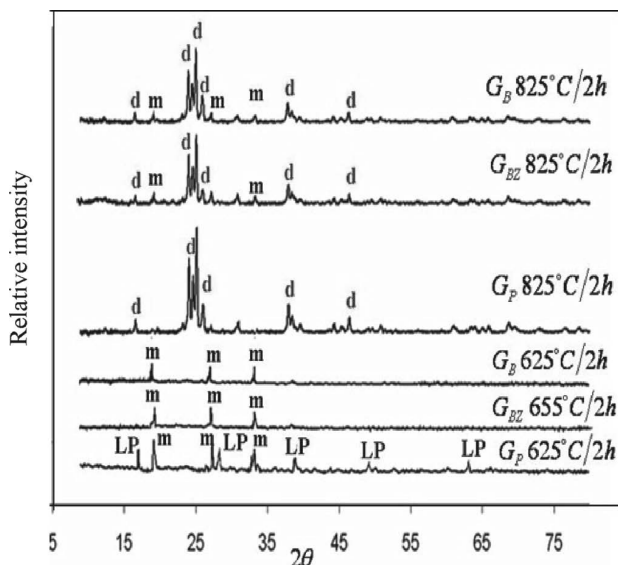


Fig. 2: XRD patterns of the glasses heat-treated for 2 h at their first and second exothermic peak temperatures of  $G_P$ , d: lithium disilicate, m: lithium meta-silicate, LP:  $Li_3PO_4$ .

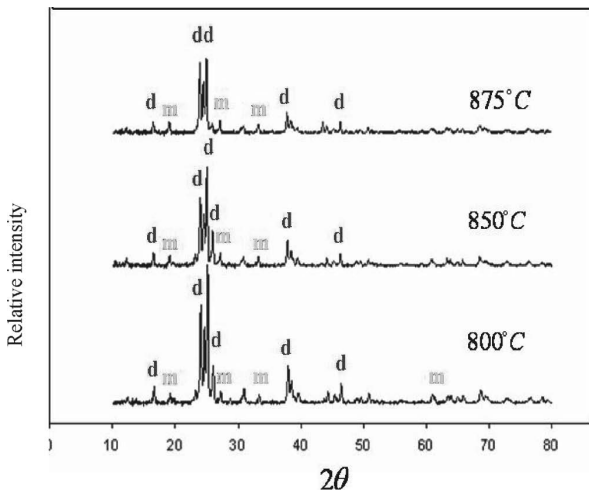
A clearly observable exothermic peak in  $G_P$  and higher intensities of its related XRD patterns indicate that bulk crystallization is probably the mechanism of crystallization for its crystalline phases. Moreover, firing of samples at 825 °C has led to a considerable reduction of  $Li_2SiO_3$  in  $G_B$  and  $G_{BZ}$  and the complete disappearance of this phase in  $G_P$ . Therefore, it can be concluded that besides surface crystallization,  $Li_2Si_2O_5$  also precipitates epitaxially on the  $Li_2SiO_3$  crystals and grows at the expense of the latter phase. The role of  $Li_2SiO_3$  as a precursor for crystallization of  $Li_2Si_2O_5$  has been mentioned by other researchers<sup>1,7</sup>.

Table 2 shows the characteristics of the three compacted glasses, after firing respectively at 800, 850, 875 and 900 °C for 2 h. These results showed that the optimum sintering temperature of  $G_P$  was 875 °C and that of the two other glasses was 800 °C. It should be noted that the latter specimens were deformed above 850 °C. It seems that a higher degree of crystallization in  $G_P$  is responsible for its higher sintering temperature.

Figs. 3, 4 and 5 show the XRD patterns of the  $G_B$ ,  $G_{BZ}$  and  $G_P$  after firing at different temperatures. It can be seen that both  $Li_2Si_2O_5$  and  $Li_2SiO_3$  are present in the  $G_B$  and  $G_{BZ}$  specimens and the amounts of these phases decrease slightly with temperature. On the other hand, apart from the specimens heat-treated at 900 °C,  $Li_2Si_2O_5$  was the only crystalline phase detected in the  $G_P$  glasses. Increasing the firing temperature to 900 °C caused a slight amount of  $Li_2SiO_3$  to recrystallize in the  $G_P$  specimen, apparently at the expense of  $Li_2Si_2O_5$ . It seems that  $Li_2Si_2O_5$  particles dissolve into the residual glass phase at higher temperatures and re-precipitate in the form of  $Li_2SiO_3$  at about 625 °C during cooling of these specimens.

**Table 2:** Sinterability of the three glasses at different temperatures.

Sintering temperature (°C)	800	850	875	900	
$G_B$	3.11	1.32	1	-	
Water absorption (%)	$G_{BZ}$	1.74	0.91	-	-
	$G_P$	5.60	2.90	0.63	0.62
Firing shrinkage (%)	$G_B$	16.00	14.40	13.98	-
	$G_{BZ}$	19.00	16.24	-	-
	$G_P$	8.11	14.02	15.50	15.12
Bulk density (g/cm <sup>3</sup> )	$G_B$	2.89	2.46	2.63	-
	$G_{BZ}$	3.05	2.83	-	-
	$G_P$	2.30	2.44	2.81	2.05
Relative density (%)	$G_B$	91.2	87.3	89.1	-
	$G_{BZ}$	90.2	89.6	-	-
	$G_P$	72.9	81.3	91.8	90.1
Porosity (%)	$G_B$	8.8	12.7	10.9	-
	$G_{BZ}$	9.8	10.4	-	-
	$G_P$	27.1	18.7	8.2	9.9



**Fig. 3:** XRD patterns of  $G_B$  specimens after firing at different temperatures, d: lithium disilicate, m: lithium metasilicate.

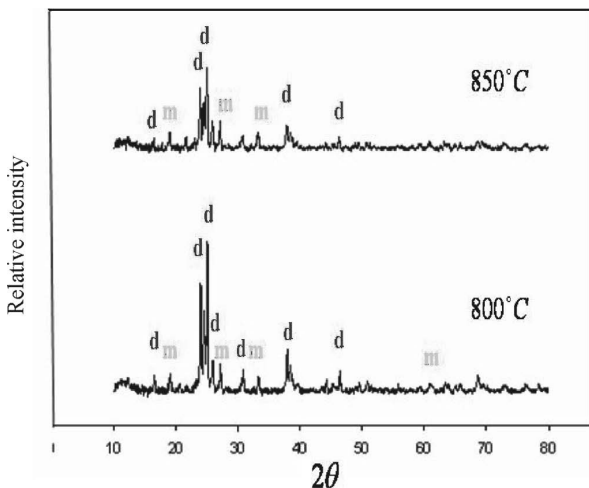


**Fig. 4:** XRD patterns of  $G_{BZ}$  specimens after firing at different temperatures, d: lithium disilicate, m: lithium metasilicate.

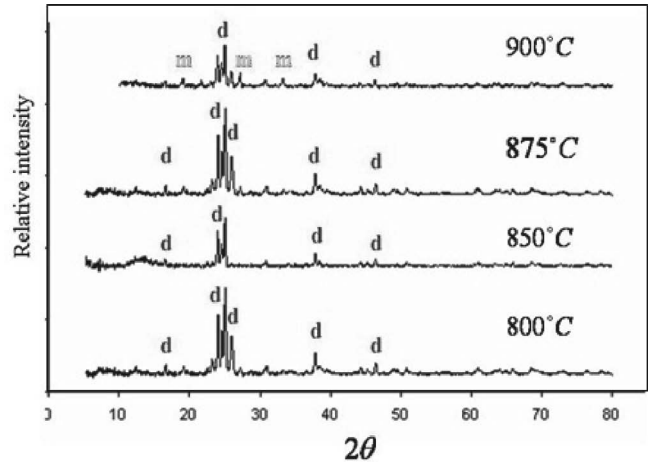


**Fig. 5:** XRD patterns of  $G_P$  specimens after firing at different temperatures, d: lithium disilicate, m: lithium metasilicate.

As the crystalline phases may be altered during hot pressing at higher temperatures, e.g. 950 °C in the usual lost wax method, the prepared glassy ingots were re-fired at the above-mentioned temperature. As it was assumed that application of pressure was ineffective in the crystallization process during re-firing, the pressure parameter was omitted in this experiment. Fig. 6 shows the XRD patterns of the re-fired glassy ingots (15 min). As it can be seen, re-firing has caused the complete conversion of lithium disilicate to lithium meta-silicate in the specimens  $G_B$  and  $G_{BZ}$ , as a result of the dissolution of the former phase into the residual glass and recrystallization in the form of lithium meta-silicate during the cooling cycle. A higher initial amount of lithium disilicate and a different residual glass composition in the ingot  $G_P$  has probably led to the saving of this phase in the re-fired  $G_P$  specimen. Lithium-disilicate-containing glass-ceramics are stronger, with regard to mechanical strength, than lithium meta-silicate-based glass-ceramics. Therefore, it seems that  $G_P$  is a more suitable composition for restorative prosthesis in respect of the mechanical properties.

(2) *Glass-ceramics microstructures*

Fig. 7 shows the microstructures of different glasses sintered at their optimum temperatures. The needle-like particles are  $Li_2Si_2O_5$  crystals. The comparison of microstructures also shows that  $G_P$ , even with its higher firing temperature, has crystalline particles smaller than 2  $\mu m$ . This observation and the presence of lithium phosphate in the XRD patterns of  $G_P$ , heat-treated at 650 °C, confirms again the earlier report<sup>6</sup> indicating that  $P_2O_5$  helps  $Li_2Si_2O_5$  crystals to precipitate more easily, through the formation of lithium phosphate, which acts as an effective nucleant for crystallization of  $Li_2SiO_3$  and subsequently  $Li_2Si_2O_5$ . Apel *et al.*<sup>12</sup> also reported that  $P_2O_5$  affects crystallization by reducing the thermodynamic barrier for nucleation of  $Li_2SiO_3$ , rather than the kinetic free energy barrier.

The microstructures of the re-fired glassy ingots are shown in Fig. 8. Accordingly, while the re-fired  $G_P$  exhibits crystalline particles smaller than 10  $\mu m$ , which according to XRD results (Fig. 6) are attributed to lithium

disilicate phase, the two other glassy ingots consist of large grown crystals of lithium meta-silicate.

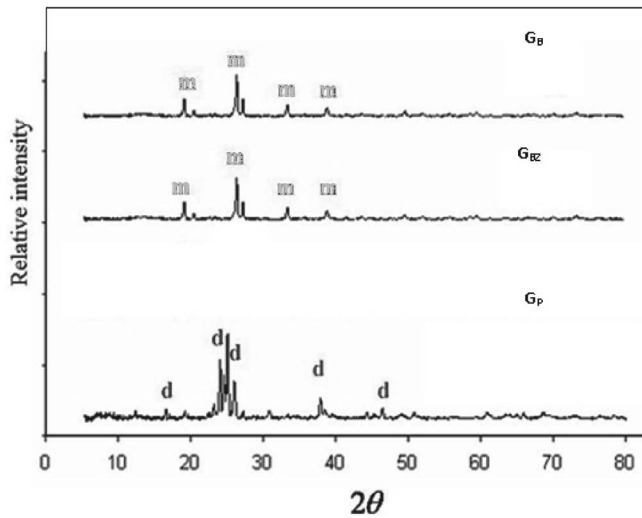


Fig. 6: XRD patterns of the ingots after re-firing at 950 °C for 15 min.

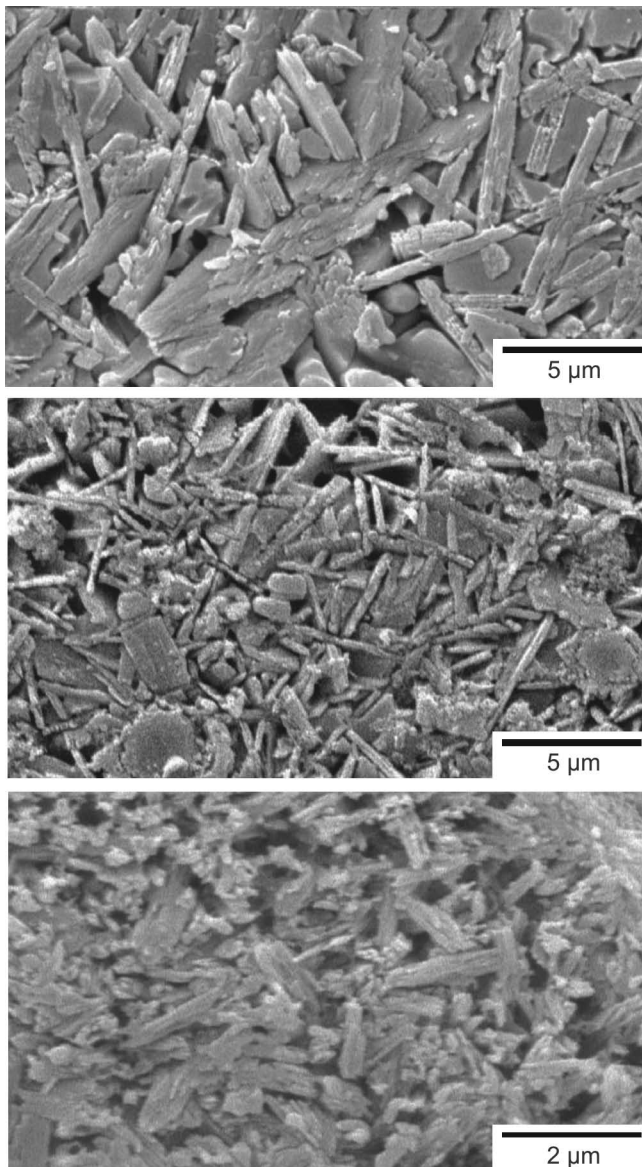


Fig. 7: Microstructures of glasses GB, GBZ and GP after firing at their optimum sintering temperatures of 800, 800 and 875 °C, respectively.

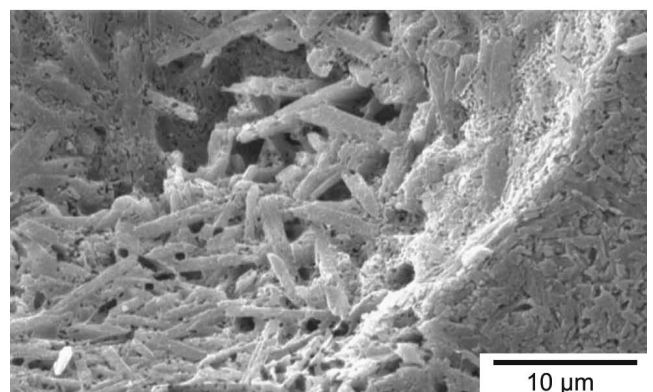
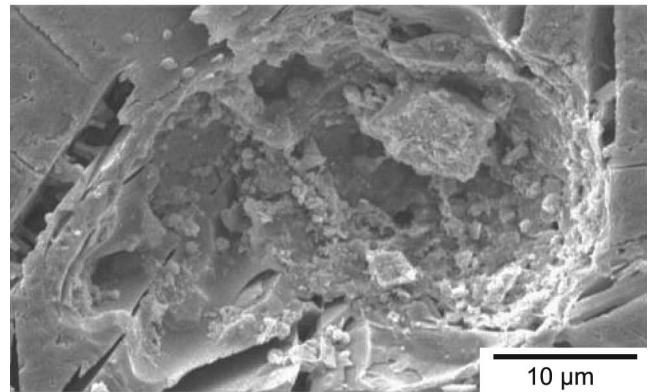
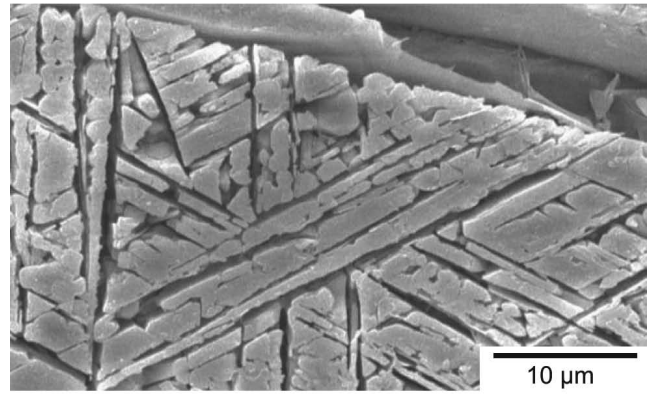


Fig. 8: Microstructures of the re-fired ingots a) GB, b) GBZ and c) GP.

#### IV. Conclusions

It was shown that while  $ZrO_2$  did not affect the crystallization behavior of the base glass, the intensity of both lithium meta-silicate and disilicate were increased with addition of  $P_2O_5$ .

Lithium phosphate was detected in the  $P_2O_5$ -containing glass after its heat treatment at the first DTA peak temperature. Lithium phosphate acted as a nucleating agent for crystallization of  $Li_2SiO_3$  and consequently  $Li_2Si_2O_5$ . Crystallization of lithium phosphate is responsible for the finer texture, higher amounts of crystalline phases and hence higher sintering temperature of the  $P_2O_5$ -containing glass.

According to the re-firing results of glassy ingots, while lithium disilicate converts to meta-silicate in the  $G_B$  and  $G_{BZ}$  specimens, it remains unchanged in the  $P_2O_5$ -containing glass composition. This means that  $P_2O_5$  is an essential constituent of glasses in the manufacture of lithium-disilicate-based glass ceramics.

## References

- 1 Höland, W., Beall, G.: Glass ceramic technology, the american ceramic society, Westerville, Ohio, 2002, 279–302.
- 2 Freiman, S.: Global roadmap for ceramic and glass technology, in Freiman, S. (Editor): The 1<sup>st</sup> International Congress in Ceramics, American Ceramic Society, Toronto, 2007, 1–13.
- 3 Anspach, O., Keding, R., Russel, C.: Oriented lithium disilicate glass-ceramics prepared by electrochemically induced nucleation, *J. Non-Cryst. Solids*, **351**, 656–62, (2005).
- 4 Morales, A.A., Pfeiffer, H., Delfin, A., Bulbulian, S.: Phase transformations on lithium silicates under irradiation, *Mater. Lett.*, **50**, 36–40, (2001).
- 5 Taskonak, B., Sertgöz, A.: Two-year clinical evaluation of lithia-disilicate-based all-ceramic crowns and fixed partial dentures, *Dent. Mater.*, **22**, 1008–13, (2006).
- 6 Monmaturapoj, N., Lawita, P., Thepsuafan, W.: Characterization and properties of lithium disilicate glass ceramics in the SiO<sub>2</sub>-Li<sub>2</sub>O-K<sub>2</sub>O-Al<sub>2</sub>O<sub>3</sub> system for dental applications, *Adv. Mat. Sci. and Eng.*, article iD 763838, (2013).
- 7 Höland, W., Rheinberger, V.M., Ritzberger, C., Apel, E.: Surface or internal nucleation and crystallization of glass-ceramics, *Opt. Mater.*, **35**, 1756–58, (2013).
- 8 Yuan, K., Wang, F., Gao, A.J., Sun, X., Deng, Z., Wang, H., Chen, J.: Effect of sintering time on the microstructure, flexural strength and translucency of lithium disilicate glass-ceramics, *J. Non-Cryst. Solids*, **362**, 7–13, (2013).
- 9 Zhao, K., Wei, Y.-R., Pan, Y., Zhang, X.-P., Swain, M.V., Guess, P.C.: Influence of veneer and cyclic loading on failure behavior of lithium disilicate glass-ceramic molar crowns, *Dent. Mater.*, **30**, 164–171, (2014).
- 10 Fernandes, H.R., Tulyngonov, D.U., Pascual, M.J., Ferria, J.M.F.: Structure-property relationships and densification-crystallization behaviours of simplified lithium disilicate glass compositions, *Ceram. Int.*, **40**, 129–140, (2014).
- 11 Zheng, X., Wen, G., Song, L., Huang, X.X.: Effect of P<sub>2</sub>O<sub>5</sub> and heat treatment on crystallization and microstructure in lithium disilicate glass ceramics, *J. Acta Mater.*, **56**, 549–58, (2008).
- 12 Apel, E., Hoen, C.V., Rheinberger, V., Höland, W.: Influence of ZrO<sub>2</sub> on the crystallization and properties of lithium disilicate glass-ceramics derived from a multi-component system, *J. Eur. Ceram. Soc.*, **27**, 1571–77, (2007).
- 13 Arvind, A., Sarkar, A., Shrikhande, V.K., Tyagi, A.K., Kothiyal, G.P.: The effect of TiO<sub>2</sub> addition on the crystallization and phase formation in lithium aluminium silicate (LAS) glasses nucleated by P<sub>2</sub>O<sub>5</sub>, *J. Phys. Chem. Solids*, **69**, 2622–27, (2008).
- 14 Lambrechts, P., Goovaerts, K., Bharadwaj, D., De Munck, J., Bergmans, L., Peumans, M., Van Meerbeek, B.: Degradation of tooth structure and restorative materials, *Wear*, **261**, 980–86, (2006).
- 15 Studart, A.R., Filser, F., Kocher, P., Luthy, H., Gauckler, L.J.: Cyclic fatigue in water of veneer-framework composites for all-ceramic dental bridges, *Dent. Mater.*, **23**, 177–85, (2007).
- 16 Höland, W., Apel, E., Hoen, C.V., Rheinberger, V.: Studies of crystal phase formations in high-strength lithium disilicate glass-ceramics, *J. Non-Cryst. Solids*, **352**, 4041–50, (2006).

